Composites: Part A 194 (2025) 108899

Contents lists available at ScienceDirect

Composites Part A

journal homepage: www.elsevier.com/locate/compositesa

Short communication

On residual tensile strength after lightning strikes

X. Xu [a,*], S.L.J. Millen [b,*], D. Mitchard [c], M.R. Wisnom [d]

[a] Centre for Aeronautics, Faculty of Engineering and Applied Sciences, College Road, Cranfield MK43 0AL, UK
[b] School of Mechanical and Aerospace Engineering, Queen's University Belfast, Ashby Building, Belfast BT9 5AH Northern Ireland, UK
[c] Morgan-Botti Lightning Laboratory, Advanced High Voltage Engineering Research Centre, School of Engineering, Cardiff University, Cardiff CF24 3AA, UK
[d] Bristol Composites Institute, University Walk, Bristol BS8 1TR, UK

ARTICLE INFO

Keywords:
Delamination
Lightning strike
Tension after Lightning Strikes (TAL)
Finite Element Analysis (FEA)

ABSTRACT

The study of post lightning strike residual strength is still relatively underdeveloped in the literature. Different approaches including in-plane compression or flexural testing have been used, but in-plane tensile loading post-strike has not been studied in detail. Although previous attempts have been made to determine the residual strength using Compression-After-Lightning (CAL) tests on composite laminates, these have been limited and not readily applicable under tensile loads. Therefore, this work completes Tension-After-Lightning (TAL) testing at 75 kA on composite laminates, a more realistic peak current than previously reported for TAL tests, to assess the knock-down in strength post-strike. The measured average TAL failure stress was 716 MPa, a reduction of 23 % from the baseline tensile failure stress of 929 MPa in the literature. This confirms a similar knock-down factor reported at lower peak currents (e.g. 50 kA), but the new TAL specimen geometry ensures that the lightning damage is contained within both the lightning and TAL specimen widths. In addition, a new Finite Element (FE) based virtual test was conducted, considering 0° ply splitting, and validated with the TAL tests herein. The TAL simulation predicted the residual tensile failure stress well, within 6 % of the measured value.

1. Introduction

The effect of lightning strikes on composite structures has been studied for a number of years, either computationally e.g. [1] or experimentally [2,3], focussing on the highest peak current Waveform A (characterised as the first return stroke of a natural lightning strike) or Waveform D (a subsequent stroke) [4]. It has been established that lightning strikes on Carbon Fibre-reinforced Polymer (CFRP) composites can produce significant damage [5]. The influence of the strike on structural performance has been quantified using visual inspection, Non-destructive Testing (NDT) methods such as X-ray Computed Tomography (CT-scans), and other techniques such as pulse thermography [6].

An informative assessment of the effect of lightning damage is through the quantification of the structure's residual strength post-strike. The study of residual strength post lightning strike has been growing in recent years with works focusing on compressive [5,7–9], flexural [10–12] and to a lesser extent Tension-After-Lightning strike (TAL) [9,13]. Tension-After-Impact (TAI) studies are more common in the literature, and some have considered laminates with scarf-repairs [14–17]. The fundamental mechanisms of failure between TAI and TAL are assumed to be similar i.e. fracture and delamination at the damage site. While Compression-After-Impact (CAI)/Compression-After-Lightning (CAL) specimens typically measure 150 mm × 100 mm, TAI testing has been completed with specimens measuring 200 mm× 50 mm [17]. To the authors best knowledge only two studies have considered TAL testing or modelling in the open literature. One experimental study used long thin specimens measuring 305 mm× 38 mm exposed to 10–50 kA variations of Waveform D [9]. However, these specimen dimensions caused lightning damage areas to reach the edges of the test specimen and did not accurately reflect the size of a typical test specimen. Feraboli and Miller [9] acknowledged that the small specimen dimensions could introduce finite-width effects relating to both the damage formation, i.e. lightning damage reached the edges, and residual strength, likely to artificially reduce the tensile strength of the specimen. The other study, focussed on FE modelling, used 10–40 kA variations of Waveform A [13], however, did not include experimental validation. As such a detailed study of TAL using repeated experiments and complimentary modelling is underdeveloped and will be addressed herein. Despite these limitations, these works were able to quantify the reduction in load carrying capacity and conclude that residual strength decreases with

* Corresponding authors.
E-mail addresses: xiaodong.xu@cranfield.ac.uk (X. Xu), scott.millen@qub.ac.uk (S.L.J. Millen).

https://doi.org/10.1016/j.compositesa.2025.108899
Received 14 December 2024; Received in revised form 17 March 2025; Accepted 29 March 2025
Available online 31 March 2025

increasing peak current, I_{peak} (kA), the rise time from 10 % to 90 % of the maximum current, T_1 (ms), or the time to reach the post-peak value of 50 % of the maximum current, T_2 (ms). Generally speaking, previous works have established that residual TAL failure stress decreases approximately linearly with peak current for unnotched specimens but shows a modest increase for filled-hole tension specimens [9,13]. However, the previous experimental studies of TAL tests did not effectively contain the strike damage in the specimen or test at more realistic peak currents above 50 kA so the tests were not representative of the situation in a real structure. The hypothesis of the work herein is that a thorough assessment of the TAL failure stress can only be determined following repeated tests at high peak current, worst-case strike conditions. While previous attempts have been made to determine the Compression-After-Lightning strike (CAL) failure stress of CFRP laminates, these have not included repeated experiments [5]. In contrast, this work, completes a combined experimental and numerical study of TAL with repeated testing on CFRP laminates to assess the knock-down in strength post-strike. In addition, a new Finite Element (FE) based virtual test framework is validated against experiments and is used to predict tensile failure initiation during TAL testing.

2. Methodology and experimental results

2.1. Lightning strike tests

A large test panel measuring 650 mm × 440 mm × 4 mm with a stacking sequence of $[45/90/\text{-}45/0]_{4s}$ was manufactured using Hexcel's HexPly® IM7/8552 carbon/epoxy pre-preg. The test panel was bolted into a grounded rig, below an electrode as shown in Fig. 1a, to ensure firm contact between the specimen and grounding clamps, forming a route to ground for the injected current. It was demonstrated previously that only a small portion of the injected current flows through the bolts to the grounding clamps due to the distance between the local attachment point and these bolts, and the bolt holes do not have a tangible effect on the residual strength of the specimen [5]. Lightning strike tests were performed at Cardiff University's Lightning Laboratory, part of the Advanced High Voltage Engineering Research Centre. A 100 μs long lightning Waveform D with a peak current of 75 kA and *T1/T2* of 18/40 μs, following the EUROCAE ED-84 standard [18], as shown in Fig. 1b, was injected into each quadrant in turn, following a previously established procedure [5]. Current injection in the centre of one quadrant allows grounding into that corner with minimal impact on the other three quadrants of the panel. In the lighting tests, a small insulating plastic diverter sphere (to prevent contamination between the electrode and the specimen) and a thin metallic fuse wire (50 mm long) were used to guide the lightning arc to the exact point at the centre of each quadrant on the panel [19]. These points in the four quadrants are far apart thus the lightning damage is not expected to overlap into neighbouring quadrants, as confirmed by the previous study [5]. Previous results showed that a full 100 kA Waveform D strike extended 90 mm wide and towards the quadrant boundary on the test panel, while a 50 kA strike generated limited lightning damage [5]. Therefore, in this work, modified 75 kA Waveform D strikes were used to produce significant damage and assess the effect of more realistic peak currents, but still allow the resulting damage to be contained within the limits of each quadrant and within the limits of the resulting TAL specimen.

2.2. Ultrasound inspection post-lightning strike

An initial visual inspection of the post-strike damage showed many broken, lifted, and separated fibres and a large amount of surface pitting around the strike area, as shown in Fig. 4a. Matrix damage (i.e., cracking or thermal decomposition) and further surface pitting was also observed a short distance from the initial lightning attachment point. The lightning struck panel was further inspected at the Bristol Composites Institute using an ultrasound scanner with a multi-format coherent receiver developed for advanced modulation format signals. The time-of-flight information is presented in Fig. 2a, indicating the extent of damage caused by the lightning strikes. The lightning damage is comparable to the previously reported CT scan image in Fig. 2b from Ref. [5], for a 75 kA Waveform D strike on the same material and stacking sequence, confirming repeatability. The scans show that the lightning damage is superficial and unsymmetrical through the thickness.

2.3. Tension-after-lightning (TAL) tests

After lightning strike testing and ultrasound scanning were complete, the panel was carefully cut into its respective quadrants using a diamond-coated disk to assess residual tensile strength. The size of each tensile specimen was 220 mm × 85 mm × 4 mm to sufficiently cover the lightning damage site in each specimen.

TAL tests were completed at the Bristol Composites Institute using an Instron 250 kN hydraulic-servo universal test machine. The tensile specimens were gripped by the test machine, leaving a gauge length of approximately 120 mm. The tests were completed under displacement control at a loading rate of 1 mm/min. The load–displacement response from all four tests is shown in Fig. 3. The response was approximately linear; however, some minor non-linearity was observed, likely because the displacements were measured at the crossheads. Small load drops were observed just prior to the ultimate failure in some tests. Gross-section stress was used to calculate the failure stress based on the nominal thickness and measured width. The average failure stress is 715 MPa (C.V. 1.3 %). This is 23 % lower than the reported pristine tensile failure stress of 929 MPa for the same material with the same stacking sequence [20]. The current test condition is also comparable to the previous [20] with a similar gauge length, test set-up, and only the width being about three times wider. This different dimension would not greatly affect the unnotched strength, because previous research has

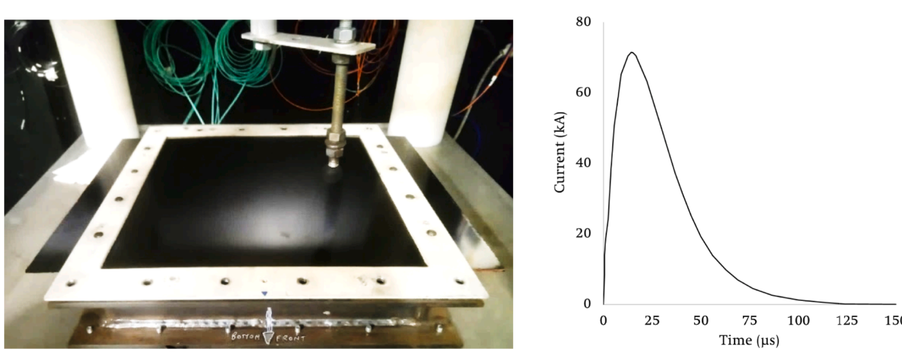

a) Clamping arrangement *b) Lightning test waveform*

Fig. 1. Laboratory lightning strike test with a) clamping used and b) waveform used.

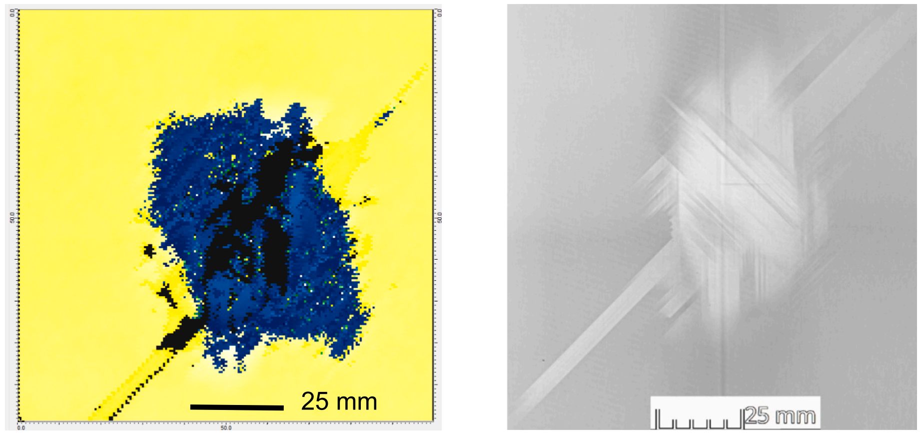

a) Ultrasound scan of a typical TAL specimen *b) CT scan of a previous CAL specimen* [5]

Fig. 2. Lightning damage in a typical specimen after lightning strikes with a 75kA peak current.

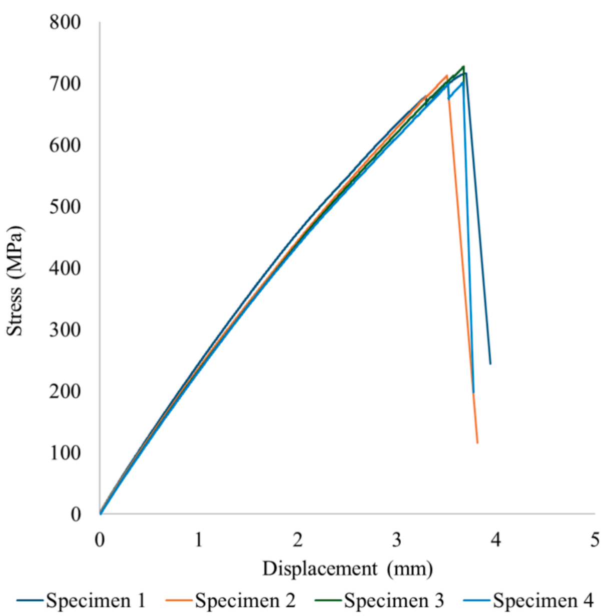

Fig. 3. Stress-displacement curves from four TAL tests.

shown that there is only a 3.4 % reduction in unnotched strength for four times increase in linear dimensions [21]. In comparison, a previous study [9] reported a drop in tensile failure stress of approximately 20 % after a 50 kA strike. However, the previous work used long, thin specimens and observed that TAL failure stress varied from approximately 120 MPa to 140 MPa with an approximate C.V. of 7.7 %. The results herein, using larger specimens containing the lightning damage within the specimen limits show that TAL failure stress varied from approximately 701 MPa to 728 MPa. Given the low C.V. of 1.3 % it can be assumed that the physical behaviours of the strike are sufficiently repeatable that further tests are not necessary.

Gauge section failure around the lightning damage site was observed in all four tensile tests, with exemplar failures shown in Fig. 4. During tensile loading the specimen failed at its centre and delamination propagated from the existing lightning strike delamination and damage regions to the specimen edges. The in-plane damage was extensive, owing to the complexity of the lightning damage pattern shown in Fig. 2. The majority of post-tension damage is observed in the upper plies which is directly correlated to the locality of severe lightning damage, discussed previously. Inspection of the specimen post-strike and post-TAL indicate that only the top few 0° plies have been damaged, which has limited the reduction in TAL failure stress to 23 %. While these results can indicate the global failure of the specimen, it is important to analyse contributions to failure and residual strength at a ply level.

3. Finite Element (FE) modelling

A virtual test framework [22], previously developed for CAL failure

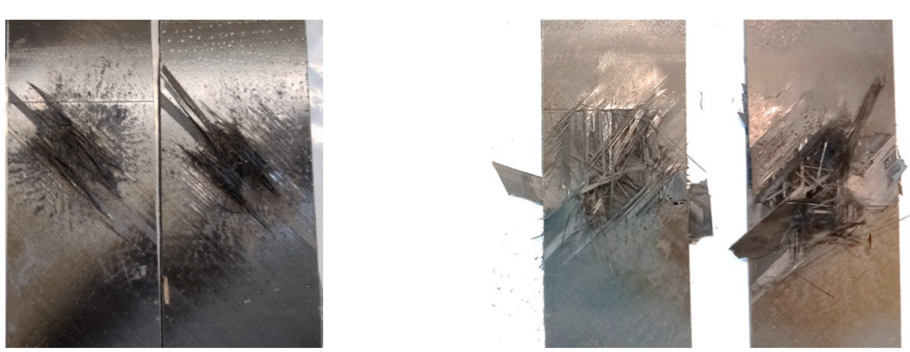

a) Post-strike, pre-TAL testing *b) Post-TAL testing*

Fig. 4. Images showing Specimens 3 and 4 (L-R) a) before TAL testing and b) after TAL with failures at the gauge section.

stress predictions, was applied to predict the TAL failure stress. Sequentially coupled thermal-electric and thermo-mechanical models were combined with TAL analyses. Thermal-electric models were used to predict thermal damage resulting from Joule or resistive heating, while thermo-mechanical models were used to predict lightning mechanical damage due to the combined effects of mechanical strain (from dynamic loading) and thermal strain (due to temperature transferred from the previous thermal damage simulation). Both the thermal-electric and thermo-mechanical models completed previously [22] measured 275 mm × 250 mm to replicate the quadrant of the larger lightning test panel. Since the TAL specimens measured 220 mm × 85 mm, the geometric size of the TAL model was reduced to match the experimental arrangement. Given the repeatability of the lightning strike damage between studies (Fig. 2), predicted thermal-electric and thermo-mechanical results presented previously were reused [22,23]. Fig. 5 compares the ultrasound scan, including an approximate outline of the overlaid damage area, with the predicted lightning mechanical damage and delamination from the thermo-mechanical simulation.

TAL simulations were completed in ABAQUS/Explicit with C3D8R elements (1.5 mm × 1.5 mm × 0.125 mm uniform, similar to Ref. [22]). In a similar manner to the thermal-electrical and thermo-mechanical models, only the first 12 plies of the TAL model were represented ply-by-ply within which the key lightning damage characteristics were transferred from Fig. 5b, using a Python script. Two forms of damage, intralaminar mechanical damage, within the ply, and interlaminar delamination, between the plies, were analysed and transferred. Areas of element deletion on each ply were chosen to represent intralaminar mechanical damage and were captured using nodal coordinates to describe the hole. These coordinates were then converted to create corresponding damaged element sets in the TAL model. A similar process was used for the transfer of delamination. In this case, areas captured by the CSDMG area (scalar damage variable for delamination) from the thermo-mechanical analysis for each ply-ply interface was used. The rest of the 20 plies were lumped into a block using homogenised properties, using the same strategy as before [22].

Along the loading direction, the TAL model was fixed at one end, while prescribed displacements were applied at the opposite end at a constant rate of 1 mm/second. Semi-automatic mass scaling was used with a target timestep of 1×10^{-6} s. Despite a higher loading rate than that in the experiments, and the use of mass scaling, there was no significant dynamic effect observed. Therefore, the TAL simulation could be considered quasi-static.

The maximum stress criterion was used to predict fibre failure, shown in Equation (1):

$$F = |\sigma|/X_t \geq 1 \tag{1}$$

When the maximum fibre-direction stress (σ) reached the tensile strength (X_t), the elements were flagged, and their fibre-direction stress was reduced to zero. This is effectively a failure initiation criterion assuming first ply failure which may give conservative predictions.

The current model is not a fully ply-by-ply model. Cohesive surfaces were defined between the first twelve plies within which lightning damage was present, and between the 12^{th} ply and the remaining 20-ply block. Within the three 0° plies of the laminate, potential splitting paths were created at the edge of the lightning fibre damage as shown in Fig. 6a. No splitting was modelled in other plies because the 0° splitting was found to be critical for predicting sharp-notched [24] and open-hole tensile failures [25] of the same material and stacking sequence. The same cohesive surface approach and properties were used for 0° splitting as for other interfaces. The properties for the cohesive surfaces used are shown in Table 1 [22].

During TAL simulation, separation of cohesive surfaces initiated and propagated from the lightning damaged area along the pre-defined splitting paths. This is demonstrated by the stress distribution in a typical 0° ply as shown in Fig. 6. Fig. 6 includes the approximate lightning fibre damage, transferred from the thermo-mechanical simulation, which is smaller than the area in Fig. 5 given Fig. 6a only shows the critical fibre damage in the 3^{rd} 0° ply while Fig. 5 shows overlaid delamination for multiple plies. Early on, high stresses occurred near the lightning damage site (Fig. 6b). As splitting and delamination grew, the high stresses spread beyond the lightning fibre damage site and their concentration was reduced (Fig. 6c). The 0° splitting and delamination are represented by the degraded cohesive surfaces (Fig. 6d). The TAL model fails from its centre near the existing lightning damage site to the model edges (Fig. 6e), but some elements to the left are also affected post failure. The delayed fibre failure initiation immediately triggered the ultimate failure in the TAL model.

The predicted TAL failure stress was 670 MPa, which is the maximum gross-section stress at the predicted failure load of 228 kN. It is only 6 % less than the measured average TAL failure stress of 716 MPa (C.V. 1.3 %). Further improvements to the TAL failure stress prediction could be achieved by using a more detailed ply-by-ply FE model, similar to Ref. [28] which considers progressive fibre failure combined with multiple 0° splitting paths parallel to the lightning damage site. It is particularly relevant for future cases with less severe lighting damage which may see more complex failure modes and prolonged damage evolution.

4. Conclusions

This work completed a combined experimental and numerical study

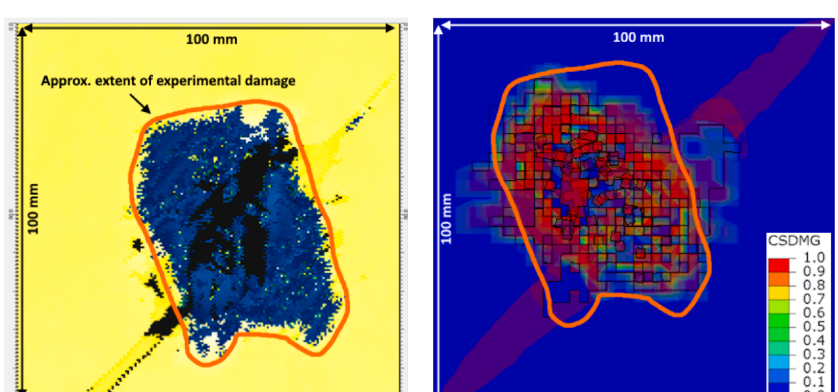

a) Ultrasound scan with outlined damage *b) Thermo-mechanical damage prediction including experimental outline*

Fig. 5. Comparison of experimental ultrasound scan and thermo-mechanical damage predictions where colours represent delamination damage.

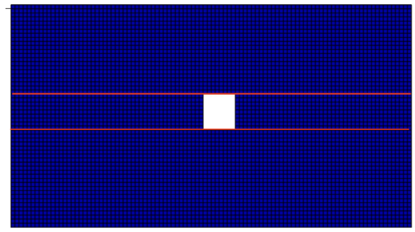

(a) Potential splitting paths (red) at the central lightning damage site

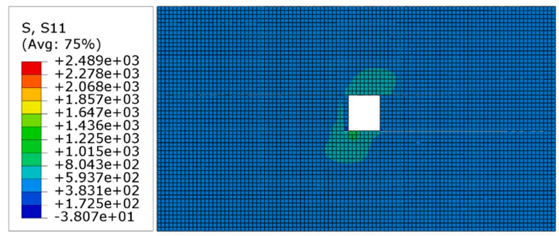

(b) Stress distribution early on

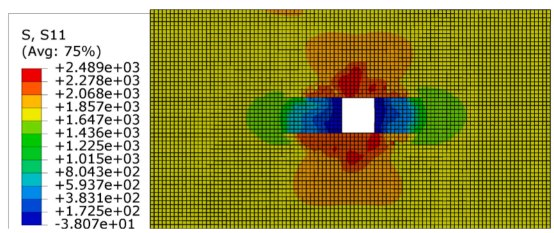

(c) Stress distribution just before failure

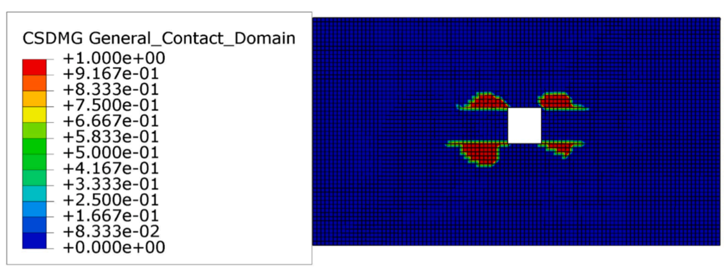

(d) Degraded cohesive surfaces just before failure

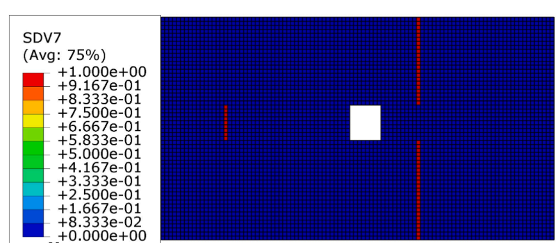

(e) Fully degraded ply elements (red) after failure

Fig. 6. FE results in the 3rd 0° ply of the TAL model.

of residual tensile strength after lightning strikes. Four repeated tests were successfully conducted on quasi-isotropic carbon/epoxy laminates. The specimens were subjected to Waveform D laboratory generated lightning strike with a 75 kA peak current, more realistic than the previously reported TAL tests. The lightning damage was extensive and unsymmetrical through the thickness, but was contained within the specimen width and so was representative of damage on a real structure. The damage resulted in a 23 % reduction from the baseline tensile failure stress reported in the literature. A new virtual test incorporating 0° splitting was validated by the Tension-After-Lightning (TAL) tests herein. The TAL simulation predicted the residual tensile failure stress well, within 6 % of the measured value. The new TAL test results and model can inform the design of lightning resistant composite structures.

CRediT authorship contribution statement

X. Xu: Writing – original draft, Visualization, Validation, Software, Resources, Project administration, Methodology, Investigation, Funding

Table 1
Material properties for IM7/8552 used in the TAL model [26,27].

Ply Material Properties						
E_1 (GPa)	$E_2 = E_3$ (GPa)	$G_{12} = G_{13}$ (GPa)	G_{23} (GPa)	$\nu_{12} = \nu_{13}$	ν_{23}	$X_{t,ply}$ (MPa)
161	11.4	5.17	3.98	0.32	0.44	2723
Homogenised Block Material Properties						
$E_1 = E_2$ (GPa)	E_3 (GPa)	G_{12} (GPa)	$G_{13} = G_{23}$ (GPa)	ν_{12}	$\nu_{13} = \nu_{23}$	$X_{t,block}$ (MPa)
61.6	13.5	23.4	4.5	0.32	0.31	929 [20]
Cohesive Interface Properties						
t_n^0 (MPa)	$t_s^0 = t_t^0$ (MPa)	G_n^C (kJ/m^2)	$G_s^C = G_t^C$ (kJ/m^2)	BK Exponent	$K_{nn} = K_{ss} = K_{tt}$ (N/mm^3)	
60	90	0.2	1.0	1.45	1.28×10^5	

acquisition, Formal analysis, Data curation, Conceptualization. **S.L.J. Millen:** Writing – review & editing, Visualization, Validation, Software, Resources, Methodology, Investigation, Funding acquisition, Formal analysis, Data curation, Conceptualization. **D. Mitchard:** Writing – review & editing, Investigation, Data curation. **M. R. Wisnom:** Writing – review & editing.

Declaration of competing interest

The authors declare that they have no known competing financial interests or personal relationships that could have appeared to influence the work reported in this paper.

Acknowledgements

Travel funding and financial support for S.L.J. Millen was provided by the Queen's University Belfast Agility Fund.

Data availability

The data that has been used is confidential.

References

[1] Zhu Y, Li Y, Sun J, Liu C, Xu X, Zhang K, et al. Lightning damage analysis of composite bolted joint structures based on thermal-electrical-structural simulation. Compos. Struct. 2024. https://doi.org/10.1016/j.compstruct.2024.118720.
[2] Xia Q, Zhang Z, Mei H, Liu Y, Leng J. A double-layered composite for lightning strike protection via conductive and thermal protection. Compos. Commun. 2020; 21. https://doi.org/10.1016/j.coco.2020.100403.
[3] Duongthipthewa A, Tian Y, Duongthipthewa O, Su Z, Zhou L. A comprehensive analysis of electric, thermal, and structural effects of lightning strikes on CFRP composites and protective strategies. Compos. Commun. 2023;44. https://doi.org/10.1016/j.coco.2023.101739.
[4] SAE International. ARP5412B: Aircraft Lightning Environment and Related Test Waveforms. Aerospace Recommended Practice 2013:63.
[5] Xu X, Millen SLJ, Lee J, Abdelal GF, Mitchard D, Wisnom MR, et al. Developing test methods for compression after lightning strikes. Appl. Compos. Mater. 2023. https://doi.org/10.1007/s10443-022-10100-w.
[6] Harrell TM, Dulieu-Barton JM, Thomsen OT. Identification of lightning strike damage severity using pulse thermography through integration of thermal data. Exp. Tech. 2024. https://doi.org/10.1007/s40799-024-00713-0.
[7] Wang FS, Yu XS, Jia SQ, Li P. Experimental and numerical study on residual strength of aircraft carbon/epoxy composite after lightning strike. Aerosp. Sci. Technol. 2018;75:304–14. https://doi.org/10.1016/j.ast.2018.01.029.
[8] Xia Q, Zhang Z, Mei H, Liu Y, Leng J. A double-layered composite for lightning strike protection via conductive and thermal protection. Compos. Commun. 2020; 21:100403. https://doi.org/10.1016/j.coco.2020.100403.
[9] Feraboli P, Miller M. Damage resistance and tolerance of carbon/epoxy composite coupons subjected to simulated lightning strike. Compos. A Appl. Sci. Manuf. 2009; 40:954–67. https://doi.org/10.1016/j.compositesa:2009.04.025.
[10] Li K, An Z, Deng J, Cheng X. Lightning ablation damage and residual bending performances of scarf-repaired composite laminates with copper mesh protection. Mech. Adv. Mater. Struct. 2024:1–15. https://doi.org/10.1080/15376494.2024.2425820.
[11] Kumar V, Yeole PS, Hiremath N, Spencer R, Billah KMM, Vaidya U, et al. Internal arcing and lightning strike damage in short carbon fiber reinforced thermoplastic composites. Compos. Sci. Technol. 2021;201. https://doi.org/10.1016/j.compscitech.2020.108525.
[12] Kumar V, Yokozeki T, Okada T, Hirano Y, Goto T, Takahashi T, et al. Polyaniline-based all-polymeric adhesive layer: an effective lightning strike protection technology for high residual mechanical strength of CFRPs. Compos. Sci. Technol. 2019;172:49–57. https://doi.org/10.1016/j.compscitech.2019.01.006.
[13] Wang FS, Ding N, Liu ZQ, Ji YY, Yue ZF. Ablation damage characteristic and residual strength prediction of carbon fiber/epoxy composite suffered from lightning strike. Compos. Struct. 2014;117:222–33. https://doi.org/10.1016/j.compstruct.2014.06.029.
[14] Feng W, Xu F, Xie W, Wang A, Ma C. Impact and tension-after-impact behaviors of scarf-repaired composite laminates: an experimental and numerical approach. Mech. Adv. Mater. Struct. 2023;30:1260–73. https://doi.org/10.1080/15376494.2022.2029983.
[15] Roeper F, Sommacal S, Compston P, Tauchner J, Wolfahrt M, Pinter G. Tension-after-impact (TAI) performance and 3D damage visualization of carbon-fiber epoxy composites with adhesively bonded patch repairs. Compos. Struct. 2023;322. https://doi.org/10.1016/j.compstruct.2023.117338.
[16] Liu B, Xu F, Qin J, Lu Z. Study on impact damage mechanisms and TAI capacity for the composite scarf repair of the primary load-bearing level. Compos. Struct. 2017; 181:183–93. https://doi.org/10.1016/j.compstruct.2017.08.087.
[17] Hoseinlaghab S, Farahani M, Safarabadi M, Nikkhah M. Tension-after-impact analysis and damage mechanism evaluation in laminated composites using AE monitoring. Mech. Syst. Sig. Process. 2023;186. https://doi.org/10.1016/j.ymssp.2022.109844.
[18] EUROCAE. Aircraft Lightning Environment and Related Test Waveforms 2103. 1997.
[19] Mitchard D, Jamoshid NS, Stone C, Haddad A. Experimental and theoretical evaluation of aluminium deflection due to lightning strikes. In: 2016 33rd International Conference on Lightning Protection (ICLP). IEEE; 2016. p. 1–6. https://doi.org/10.1109/ICLP.2016.7791428.
[20] Wisnom MR, Khan B, Hallett SR. Size effects in unnotched tensile strength of unidirectional and quasi-isotropic carbon/epoxy composites. Compos. Struct. 2008;84:21–8. https://doi.org/10.1016/j.compstruct.2007.06.002.
[21] Xu X, Wisnom MR, Chang K, Hallett SR. Unification of strength scaling between unidirectional, quasi-isotropic, and notched carbon/epoxy laminates. Compos. A Appl. Sci. Manuf. 2016;90:296–305. https://doi.org/10.1016/j.compositesa:2016.07.019.
[22] Millen SLJ, Xu X, Lee J, Mukhopadhyay S, Wisnom MR, Murphy A. Towards a virtual test framework to predict residual compressive strength after lightning strikes. Compos. A Appl. Sci. Manuf. 2023;174. https://doi.org/10.1016/j.compositesa:2023.107712.
[23] Millen SLJ, Xu X, Lee J, Murphy A. A Virtual Test Framework for Residual Compressive and Tensile Strength Predictions after Lightning Strikes. 21st European Conference on Composite Materials (ECCM21), Nantes: 2024.
[24] Xu X, Wisnom MR, Li X, Hallett SR. A numerical investigation into size effects in centre-notched quasi-isotropic carbon/epoxy laminates. Compos. Sci. Technol. 2015;111:32–9. https://doi.org/10.1016/j.compscitech.2015.03.001.
[25] Hallett SR, Green BG, Jiang WG, Wisnom MR. An experimental and numerical investigation into the damage mechanisms in notched composites. Compos. A Appl. Sci. Manuf. 2009;40:613–24. https://doi.org/10.1016/j.compositesa:2009.02.021.
[26] McQuien JS, Hoos KH, Ferguson LA, Iarve EV, Mollenhauer DH. Geometrically nonlinear regularized extended finite element analysis of compression after impact in composite laminates. Compos. A Appl. Sci. Manuf. 2020;134. https://doi.org/10.1016/j.compositesa:2020.105907.
[27] Hexcel. HexTow Laminate Properties in HexPly® 8552 n.d. https://www.hexcel.com/Products/Resources/1664/hextow-laminate-properties-in-hexply-8552 (accessed December 9, 2024).
[28] Xu X, Wisnom MR, Hallett SR. Deducing the R-curve for trans-laminar fracture from a virtual Over-height Compact Tension (OCT) test. Compos. A Appl. Sci. Manuf. 2019;118:162–70. https://doi.org/10.1016/j.compositesa:2018.12.027.